

In search of a driver for atrial fibrillation

van Staveren, Lianne N.; Taverne, Yannick J.H.J.; Hendriks, Richard; de Groot, Natasja M.S.

DOI

[10.1016/j.hrthm.2025.05.024](https://doi.org/10.1016/j.hrthm.2025.05.024)

Publication date

2025

Document Version

Final published version

Published in

Heart Rhythm

Citation (APA)

van Staveren, L. N., Taverne, Y. J. H. J., Hendriks, R., & de Groot, N. M. S. (2025). In search of a driver for atrial fibrillation. *Heart Rhythm*, 22(10), e978-e989. <https://doi.org/10.1016/j.hrthm.2025.05.024>

Important note

To cite this publication, please use the final published version (if applicable). Please check the document version above.

Copyright

Other than for strictly personal use, it is not permitted to download, forward or distribute the text or part of it, without the consent of the author(s) and/or copyright holder(s), unless the work is under an open content license such as Creative Commons.

Takedown policy

Please contact us and provide details if you believe this document breaches copyrights. We will remove access to the work immediately and investigate your claim.



In search of a driver for atrial fibrillation

Lianne N. van Staveren, MD,¹ Yannick J.H.J. Taverne, MD, PhD,² Richard Hendriks, PhD,³
Natasja M.S. de Groot, MD, PhD^{1,3}

ABSTRACT

BACKGROUND Short atrial fibrillation cycle lengths (AFCLs) and regular activation patterns are associated with drivers of atrial fibrillation, although the relation with underlying patterns of activation is incompletely understood. Previous studies used automated assessment of electrograms to determine fast and regular fibrillatory rates.

OBJECTIVE We investigated the relation among AFCL, temporal variation in AFCL, and the occurrence of driver-like patterns of activation using high-density local activation time mapping.

METHODS High-density epicardial mapping of the right atrium and left atrial ventricular groove including Bachmann's bundle was performed in 71 patients admitted for elective cardiac surgery. Recording sites with the shortest median AFCL or the smallest standard deviation of AFCL were identified. Patterns of activation included focal or rotational activation, smooth propagation, propagation with conduction block (CB), collision, and remnant activity.

RESULTS There was a higher number of fibrillation waves with CB (81% [interquartile range (IQR) 76%–85%] vs 74% [68%–76%]; $P < .001$) and fractionated potentials (22% [12%–37%] vs 12% [9%–15%]; $P < .001$) at shortest median AFCL than at other recording sites. Smallest standard deviation sites harbored more smoothly propagating waves (33% [24%–54%] vs 17% [11%–25%]; $P < .001$) and a higher proportion of single potentials (76% [60%–89%] vs 59% [54%–65%]; $P < .001$). Both highly regular and fastest reactivated sites did not correspond to the origin of (repetitive) focal fibrillation waves.

CONCLUSION During extensive mapping, the fastest or most regularly activated areas are characterized by CB and smoothly propagating fibrillation waves instead of repetitive occurrence of focal or rotational activation patterns. This study rejects the concept of detecting drivers by identifying the fastest or most regularly activated recording sites.

KEYWORDS Atrial fibrillation; Mapping; Drivers; Atrial fibrillation cycle length; Irregularity

(Heart Rhythm 2025;22:e978–e989) © 2025 Heart Rhythm Society. This is an open access article under the CC BY license (<http://creativecommons.org/licenses/by/4.0/>).

Introduction

The mechanisms underlying persistent atrial fibrillation (AF) remain incompletely understood, resulting in only moderate success rates of ablation therapy ([Supplementary Table 1](#)).¹ Consequently, there is increasing interest in the concept of substrate-based ablation therapies for the more persistent types of AF.² In endocardial, epicardial, or noncontact mapping approaches, so-called focal and rotational drivers of AF have been identified using complex fractionated atrial electrograms,³ dominant frequencies and organization indexes,⁴ phase singularities,^{5,6} and/or QS morphology with frequency

gradients.⁷ However, clinical mapping studies targeting either complex fractionated atrial electrograms⁸ or dominant frequencies⁹ have not improved arrhythmia-free survival. In addition, it was demonstrated that phase singularities are not specific to driver-like patterns of activation but are often found near lines of conduction block (CB).¹⁰ These results indicate that either the mapping approaches are not sensitive or specific enough to detect drivers or the existence or importance of these driver-like patterns of activation is overestimated.

Focal or rotational drivers may give rise to fast and regular activity close to the driver's origin that degrades into irregular

From the ¹Department of Cardiology, Erasmus Medical Center, Rotterdam, The Netherlands, ²Department of Cardiothoracic Surgery, Erasmus Medical Center, Rotterdam, The Netherlands, and ³Department of Microelectronics, Signal Processing Systems, Faculty of Electrical Engineering, Mathematics and Computer Sciences, Delft University of Technology, Delft, The Netherlands.

activity—or fibrillatory conduction—further from the source. Therefore, substrate-based ablation is often focused on parameters that reflect the spatiotemporal dispersion of fibrillatory rate.¹¹ In addition, several small-scale, limited-density endocardial mapping studies identified repetitive patterns of focal and rotational activation in patients with AF and suggested that these sites represent driver-like activity and can be detected by identifying the most regularly activated areas using local activation time (LAT) mapping.^{12,13} To further explore the relation between spatiotemporal dispersion of fibrillation cycle length and patterns of activation, we used high-density LAT epicardial mapping to study driver-like activation patterns and their repetitiveness. To this end, we investigated whether areas of short AF cycle length (AFCL) and temporal variation in fibrillation intervals assessed at a high-resolution scale can be used to identify focal or rotational activity driving the fibrillatory process in patients with different AF subtypes.

Methods

Study population

The study population consisted of adult patients scheduled for elective cardiac surgery for the correction of ischemic, valvular, or congenital heart disease. Patients with a history of AF were eligible for inclusion. Exclusion criteria included previous ablative therapy or cardiac surgery, the presence of accessory atrioventricular pathways, radiation therapy of the chest, atrial pacing, severely impaired left ventricular function (ejection fraction <30%), an estimated glomerular filtration rate of <30 mL/min, and recent treatment with amiodarone. This study was approved by the Medical Ethical Committee at the Erasmus Medical Center in Rotterdam, The Netherlands (MEC-2010-054 and MEC-2014-393). The research reported in this paper adhered to guidelines as specified in the Declaration of Helsinki as revised in 2013.

Mapping procedure

High-resolution epicardial mapping was performed in all patients before cardioplegic arrest.¹⁴ A bipolar electrode was temporarily connected to the terminal crest, and a steel wire was attached to the sternum as an indifferent electrode. Mapping arrays contained an electrode grid of 128 electrodes ($n = 13$, electrode spacing 2 mm, electrode diameter 0.65 mm) or 192 electrodes ($n = 58$, electrode spacing 2 mm, electrode diameter 0.45 mm). The surgeon followed a predefined mapping scheme to map the epicardial surface of the right atrium (RA), anterior left atrio-

ventricular groove (LAVG), pulmonary vein (PV) area, and Bachmann's bundle (BB).¹⁵ Anatomic nomenclature was used conforming to recommendations by Anderson and colleagues.¹⁶ At each mapping location, 10 seconds of atrial unipolar electrograms (U-EGM) was recorded together with lead I of the surface electrocardiogram at a sampling frequency of 1000 Hz. Signals were amplified (gain 1000), filtered (bandwidth 0.5–400 Hz), analog-to-digital converted (16 bits), stored on a hard disk, and analyzed offline. When AF was not spontaneously present, it was induced by 10-second pacing bursts at the high RA.

Data analysis

LATs, defined as the moment of the steepest negative deflection of the unipolar potential, were automatically identified and annotated using customized software.¹⁵ The minimum thresholds for annotation included a peak-to-peak amplitude and slope exceeding >0.03 mV and -0.05 mV/ms, respectively. As previously defined, a refractory period of 50 ms was implemented to avoid overdetection of LATs owing to the presence of fractionated potentials.¹⁷ Two experienced investigators manually removed erroneous annotations owing to baseline drift, noise, artifacts, or ventricular far field activity. Isochronal maps and wave trajectories of fibrillation waves were reconstructed in color-coded maps using LAT.¹⁸ Fibrillation intervals, defined as the time between 2 consecutive LATs, were also manually checked for accuracy if they were shorter than 100 ms or exceeded the median fibrillation interval by 1.5-fold. Long intervals were accepted if (1) an unambiguous isoelectric line separated consecutive potentials or (2) the long interval was embedded in an isolated area surrounded by electrodes, which were activated during this interval. Long intervals at the borders of the mapping array were automatically excluded from analysis to avoid false-positive long intervals owing to a temporary loss of contact.

Analysis of fibrillatory rate and AFCL variability

Histograms were constructed consisting of all recorded fibrillation intervals. The median AFCL (mAFCL) was calculated for each electrode to determine local fibrillation rates. Temporal variability in fibrillation intervals was defined as the standard deviation (SD) of all fibrillation intervals recorded (SD AFCL) at each individual electrode. To identify repetitive focal or rotational activity, patterns of activation were assessed at recording sites (electrodes) that harbored (1) the shortest mAFCL ($mAFCL_{min}$) and/or (2) the smallest SD (SD_{min}) AFCL of a studied region when calculated from 10-second segments of U-EGM.

Classifying patterns of activation

Each LAT was assigned to a specific pattern of activation including the origin of a focal fibrillation wave, rotational pattern of activation, smoothly propagating fibrillation waves, fibrillation wave with inter- or intrawave CB, collision of wavefronts, and remnant activity. Remnant activity was defined as

Abbreviations

AF: atrial fibrillation
AFCL: atrial fibrillation cycle length
CB: conduction block
LAT: local activation time
LAVG: left atrioventricular groove
$mAFCL_{min}$: shortest median atrial fibrillation cycle length
SD AFCL: standard deviation of recorded fibrillation intervals
SD_{min} : smallest standard deviation
U-EGM: unipolar electrogram

fibrillation waves that were traceable across fewer than 4 electrodes. Therefore, all other patterns of activation required fibrillation waves propagating toward at least 3 other electrodes. Driver-like activation consisted of a recurrent pattern of focal or re-entrant activation. The origin of a focal fibrillation wave was defined as LATs completely surrounded by activations later in time.¹⁹ In addition, to correct for discontinuous conduction from nearby electrodes, a time delay of at least 40 ms was required between the focal activation starting point and previous adjacent activations, consistent with other mapping studies.^{18,19}

Re-entrant activation is defined as continuous repetitive propagation of a wavefront that returns to its origin to reactivate its own pathway.²⁰ Repetitive re-entry requires at least 2 subsequent instances of full rotation conforming to definitions applied in previous clinical work.²¹ Thus, one fibrillation wave must activate at least 1 recording site 3 times during consecutive activations before the activation pattern is regarded as 2 completed circuits.

Re-entrant fibrillation waves were independently confirmed by reassessment of the activation maps by 2 experienced investigators.

Smoothly propagating fibrillation waves refer to fibrillation waves propagating toward at least 6 of 8 adjacent electrodes with an interelectrode conduction time of ≤ 11 ms, consistent with criteria used to distinguish normal or delayed activation from lines of CB (conduction time > 11 ms) in previous studies.^{18,19} To prevent overestimation of the amount of CB of a fibrillation wave, CB (conduction time > 11 ms) occurred in at least 2 directions to be considered as a *fibrillation wave with inter- or intrawave CB*. *Wavefront collision* was recognized when 2 fibrillation waves terminated at adjacent electrodes with a conduction time of ≤ 2 ms. *Repetitive focal fibrillation waves* were defined as a series of 2 or more consecutive focal fibrillation waves. The proportion of focal fibrillation waves was defined as the number of focal fibrillation waves relative to the total number of fibrillation waves. To avoid underdetection of focal fibrillation waves at mAFCL_{min} or SD_{min} sites owing to minor shifts of the wavefront origin in relation to the mapping array, focal fibrillation waves occurring at 1 of the 8 neighboring electrodes were also assigned to the same series of focal fibrillation waves.

Assessing the degree of potential fractionation

The degree of potential fractionation in U-EGMs was assessed at recording sites harboring mAFCL_{min}, SD_{min}, and repetitive focal or rotational activity to investigate the relation between U-EGM morphology and the occurrence of different patterns of activation. Potential complexity was determined by the number of negative deflections; single potentials consisted of 1 negative deflection, short and long double potentials consisted of 2 negative deflections (≤ 15 ms or > 15 ms between deflections, respectively), and complex fractionated potentials consisted of 3 or more negative deflections. The number of fractionated potentials were calculated relative to the total amount of U-EGM potentials recorded.

Statistical analysis

IBM SPSS Statistics for Windows version 25 (IBM Corp, Armonk, NY) was used for the statistical analyses. Normally distributed continuous data are reported as average \pm SD and assessed using Student *t* test. Skewed data are reported as median (interquartile range), and for comparison of the distribution of continuous data between 2 or more subcategories, we used Kruskal-Wallis tests. In addition, we performed chi-square tests to compare categorical data (expressed as proportions). Only patients in whom mapping data of sufficient quality could be acquired from at least 3 atrial regions were included to identify predilection sites for mAFCL_{min}, SD_{min}, and the longest series of repetitive focal fibrillation waves. Signed-rank tests were performed to compare the occurrence of fractionated potentials and patterns of activation at mAFCL_{min}, SD_{min}, and sites harboring maximum repetition of focal fibrillation waves with the occurrence of fractionated potentials and patterns of activation at the remainder of the recording sites in the same patient. A 2-sided *P* value of $\leq .05$ was considered statistically significant. For comparison of fractionated potentials and patterns of activation, required *P* values for statistical significance were Bonferroni adjusted (fractionated potentials *P* $< .0125$ [ie, 0.05/4 fractionation subtypes] and patterns of activation *P* $< .008$ [ie, 0.05/6 prespecified patterns of activation]).

Results

Study population

Patient characteristics are presented in Table 1. Patients (N = 71; age, 69 ± 9 years) were predominantly male (n = 54 [75%]) and had a history of paroxysmal AF (n = 28), persistent AF (n = 26), or longstanding persistent AF (n = 17). Median time since AF diagnosis was 1.64 years (0.59–7.13). In most patients (67%), the LA was enlarged (left atrial volume index, 47 ± 24 mL/m²). AF was spontaneously present at the start of the mapping procedure in 46 patients (65%); in other patients, AF was electrically induced.

Mapping database

In total, 93,240 recording sites were assessed, including 1350 recording sites (1075–1514) per patient. Owing to low signal-to-noise ratio or artifacts, $15\% \pm 8\%$ of the recording sites were excluded from the analysis. mAFCL was 106 ms (range, 79–241 ms), and median SD was 35 ms (range, 8–60 ms).

Localizing AF drivers: Short fibrillation intervals

The distribution of mAFCL throughout the right and left atria including Bachmann's bundle in 4 different patients with AF is presented in Figure 1. As can be seen in these mAFCL maps, the mAFCL_{min} sites are not always confined to a circumscribed area but may be dispersed across multiple regions. Recordings from each mAFCL_{min} site—the fastest activated site indicated by a dotted circle—illustrate unipolar AF potential morphology encountered at these sites. Please note that recordings from these mAFCL_{min} sites display mainly fractionated potentials.

Table 1 Baseline characteristics of the study population (N = 71)

Patient characteristics	
Age, y	69 ± 9
Gender (female), n (%)	18 (25)
Risk factors	
- BMI, kg/m ²	28 ± 5
- Diabetes mellitus, n (%)	19/70 (27)
- Hypertension, n (%)	43/70 (61)
Underlying heart disease	
- IHD	7 (10)
- VHD	45 (63)
- VHD + IHD	9 (13)
- CHD	10 (14)
History of myocardial infarction, n (%)	9 (13)
AF subtype, n (%)	
- Paroxysmal	27 (39)
- Persistent	26 (36)
- Longstanding persistent	18 (23)
Time since AF diagnosis, y	1.64 [0.59–7.13]
LA enlargement, n (%)	
- Not dilated	23/67 (34)
- Mildly dilated	8/67 (12)
- Moderately dilated	6/67 (9)
- Severely dilated	30/67 (45)
LAVI, mL/m ²	47 ± 24
LV function, n (%)	
- Normal	54 (76)
- Mild impairment	15 (21)
- Moderate impairment	2 (3)
Antiarrhythmic drugs, n (%)	
- Class I	2 (3)
- Class II	48 (68)
- Class III	7 (10)
- Class IV	1 (1)
- Digoxin	13 (18)
Procedural characteristics	
AF at start of procedure, n (%)	
Mapping array, n (%)	46 (65)
192 electrodes	58 (82)
128 electrodes	13 (18)

Values are presented as number (%) and mean ± standard deviation or numbers in brackets is interquartile range.

AF = atrial fibrillation; ARB = angiotensin receptor blockers; BMI = body mass index; CHD = congenital heart disease; IHD = ischemic heart disease; LA = left atrium; LAVI = left atrial volume index; VHD = valvular heart disease.

The distribution of mAFCL_{min} for each patient separately is presented in Figure 2; mAFCL_{min} ranged from 65 to 183 (median, 93) ms and was most frequently found in the pulmonary veins region (pulmonary veins 47%, right atrium 22%, Bachmanns bundle 14%, LAVG 22%; chi-square goodness of fit $P < .001$). In only 1 patient (patient study identity 33), the same mAFCL_{min} was located at 2 distinct regions: pulmonary veins and Bachmanns bundle. However, mAFCL_{min} sites were small and covered 1 electrode (range, 1–3).

Localizing AF drivers: Regular activation

Figure 3 demonstrates the distribution of SD AFCL in the same 4 patients as depicted in Figure 1. Areas of regular activation were detected at various atrial regions. Comparison of the SD AFCL with corresponding AFCL maps reveals that short mAFCL areas are irregularly activated and thus do not

correspond to the lowest SD areas. In the entire patient group, fibrillation intervals at the fastest activated sites were indeed irregular (SD AFCL at mAFCL_{min}, 46 ms [40–55]).

Figure 4 summarizes for each patient separately the SD_{min} per atrial region to identify the most regularly activated areas. In the entire patient population, the most regularly activated sites had a median SD_{min} of 10 ms (range, 1–15) and covered 4 electrodes (range, 1–59). The most regularly activated area was most frequently located along the LAVG (LAVG 52%, right atrium 27%, pulmonary veins 19%, Bachmanns bundle 13%; $P < .001$); in 7 patients, SD_{min} was found in 2 distinct mapping regions.

Are short AFCL indicative of focal activation?

To determine whether the fastest activated sites harbor AF drivers, underlying patterns of activation at these sites were analyzed. The occurrence of the various patterns of activation at the fastest activated and most regularly activated sites for the entire patient group is presented in Table 2. Focal patterns of activation did not occur more frequently at mAFCL_{min} and SD_{min} sites than in the remainder of the atria (at mAFCL_{min}, 2% [interquartile range (IQR) 1%–3%] vs 2% [2%–3%], $P = .322$; and at SD_{min}, 0% [0%–3%] vs 1% [0%–2%], $P = .105$). Notably, none of these recording sites represented the area with the largest proportion of focal fibrillation waves for the specific patients. The largest proportion of focal fibrillation waves was 18% (12%–24%), and mAFCL_{min} and SD_{min} were not located at these sites.

Both the numbers of fibrillation waves with CB and remnant activity were increased at fastest activated sites compared with other recording sites (CB, 81% [76%–85%] vs 74% [68%–76%], $P < .001$; remnant activity, 13% [7%–20%] vs 7% [5%–10%], $P < .001$). Consequently, the number of smoothly propagating fibrillation waves at fastest activated sites was reduced (at mAFCL_{min} 3% [0%–7%] vs 17% [11%–25%]; $P < .001$).

In contrast, at the most regularly activated domains, fibrillation waves were more frequently classified as smoothly propagating fibrillation waves than at other recording sites (at SD_{min} 33% [24%–54%] vs 17% [11%–25%]; $P < .001$), whereas fibrillation waves with CB or remnant activity occurred less often (CB, SD_{min} 64% [47%–73%] vs 75% [68%–79%], $P < .001$; and remnant activity, SD_{min} 1% [0%–3%] vs 7% [5%–10%], $P < .001$). Wavefront collision was rarely observed at any of the recording sites (proportion of collision at mAFCL_{min}, SD_{min}, and other recording sites: all 0% [0%–0%], both comparisons $P < .001$).

Electrogram complexity at rapidly or regularly activated recording sites

As expected, electrogram complexity was increased at the fastest activated sites. Compared with at other recording sites, we found a larger proportion of long double potentials (16% [11%–21%] vs 12% [10%–14%]; $P < .001$) and fractionated potentials (22% [12%–37%] vs 12% [9%–15%]; $P < .001$) and a smaller proportion of single potentials (46%

Median AFCL

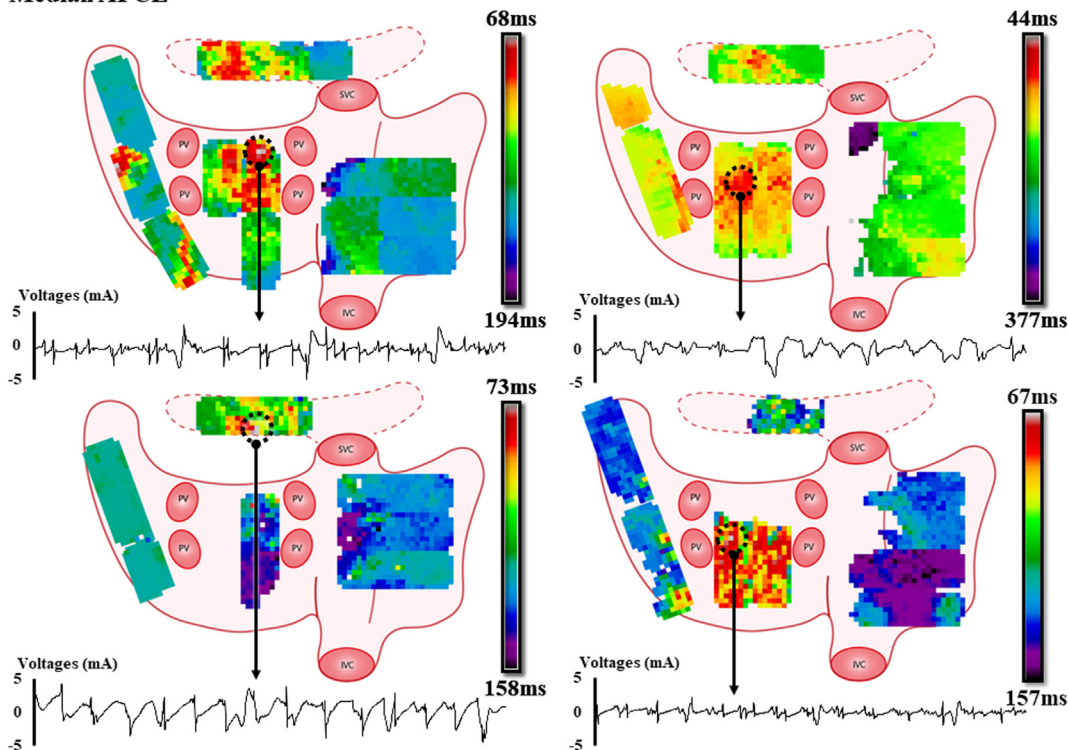


Figure 1

Distribution of mAFCL in 4 patients. Schematic representation of the atria depicting the mAFCL for each recording site separately. The relative shorter mAFCL for each patient may be confined to a single region (lower left panel) but may also be dispersed throughout multiple atrial regions such (upper left panel). The fastest activated recording sites—with the shortest mAFCL—are indicated by dotted circles. Samples of electrogram recordings from each fastest activated site are displayed (duration 2 seconds), illustrating that recordings from these fastest activated sites display mainly fractionated potentials. AFCL = atrial fibrillation cycle length; IVC = inferior caval vein; mAFCL = median atrial fibrillation cycle length; PV = pulmonary vein; SVC = superior caval vein.

[35%–58%] vs 60% [56%–65%]; $P < .001$) and short double potentials (10% [6%–14%] vs 15% [14%–17%]; $P < .001$).

At the most regularly activated sites, especially the proportion of single potentials was higher than at other recording sites (76% [60%–89%] vs 59% [54%–65%]; $P < .001$). Consequently, there was a reduced frequency of long double potentials (3% [1%–7%] vs 12% [10%–14%]; $P < .001$) and fractionated potentials (2% [1%–7%] vs 12% [9%–15%]; $P < .001$). The proportions of short double potentials did not differ (16% [7%–23%] vs 16% [14%–18%]; $P = .076$).

In search of repetitive focal activation

In each patient, we identified the areas with the highest proportion of focal fibrillation waves. The highest proportion of focal fibrillation waves ranged from 8% to 89% (median, 19%) and was most frequently located at the right atrium or LAVG (right atrium 49%, LAVG 44%, Bachmanns bundle 16%, pulmonary veins 10%; $P = .001$). These percentages correspond to a median of 10 focal fibrillation waves (range, 3–50) occurring at the same recording site for 10 seconds, although they were not always consecutive. The median total number of fibrillation waves at these recording sites was 60 (range, 51–71).

We additionally calculated the repetitiveness of all focal fibrillation waves; the histogram in Figure 5 shows the maximum number of repetitive focal fibrillation waves for each patient. The longest series of consecutive focal

fibrillation waves ranged from 2 to 28 (median, 3) and occurred most frequently along the LAVG and RA (LAVG 57%, right atrium 57%, Bachmanns bundle 21%, pulmonary veins 21%; $P < .001$). A maximum series of 3 or less consecutive focal waves were frequently recorded in multiple regions (maximum 3 distinct regions) in each patient. A series of at least 4 consecutive focal fibrillation waves ($N = 25$) were detected at the right atrium ($n = 8$), LAVG ($n = 14$), Bachmanns bundle ($n = 1$), or pulmonary veins ($n = 1$) and in 1 case at 2 regions (4 repetitions at both right atrium and LAVG). The longest series of focal fibrillation waves did not differ in length among AF subtypes (maximum number of consecutive focal waves, paroxysmal AF 3 [2–14], persistent AF 3 [2–28], long-standing persistent AF 4 [2–18]; $P = .42$).

In none of the 63 patients, the longest series of repetitive focal fibrillation waves was recorded at the fastest activated site. In 2 patients (4%), the longest series of repetitive focal fibrillation waves were located in an SD_{\min} area. In 1 of these patients, the maximum number of 2 consecutive focal fibrillation waves was located in the SD_{\min} area (SD , 13 ms) along the LAVG covering 8 electrodes, although, in the same patient, repetitions of 2 focal fibrillation waves were also detected at the Bachmanns bundle, pulmonary veins, and right atrium. In the other patient, 5 consecutive focal fibrillation waves were detected along the LAVG, in an SD_{\min} area (SD , 10 ms) that covered 59 electrodes.

PID	RA	BB	LAVG	PV
1	X	X	X	X
2	169	238	110	96
3	108	139	99	
4	110	116	151	
5	108	140	112	105
6	190	204	217	181
7	114	108	92	95
8	239	246	243	167
9	100	60	95	104
10	137	106	106	98
11	208		106	211
12	93	103	155	167
13	107	126	172	110
14	144	100	99	109
15	97	254	119	86
16	209		208	183
17	139	110	217	107
18	135	102	135	145
19	60	115	64	94
20	111	74	145	87
21	97	91		132
22	92	91	94	101
23	166	98	89	104
24	128		137	89
25	92	111	91	88
26	124	126	189	
27	92		155	85
28	X	X	X	X
29	131	118	176	170
30	200	86	95	104
31	X	X	X	X
32	116	128	92	99
33	120	140	89	89
34	91	93		141
35	X	X	X	X
36	96	143	108	102
37	112	153	91	92
38	119	108	85	82
39	160	134	119	114
40	112	92	122	100
41	176	111	182	
42	119		106	122
43	111	101	121	
44	108	121	123	106
45	108	95	93	92
46	109	103	139	92
47	121	141	145	89
48	119	94	126	82
49	105	99	90	83
50	113	85	117	85

PID	RA	BB	LAVG	PV
51	92	87	111	83
52	101	124	172	93
53	92	90	104	79
54	112	139	150	130
55	92	148		80
56	110	91	144	151
57	X	X	X	X
58	110		99	81
59	127	106	91	75
60	121	88	85	190
61	120	130	94	110
62	109	136	141	92
63	112	111	103	108
64	100	91	92	86
65	123			130
66	130	127	90	
67	X	X	X	X
68	135		140	80
69	X	X	X	X
70	99	100	151	85
71	93	98	128	96

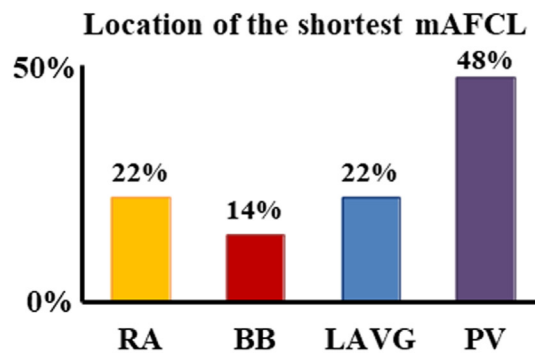
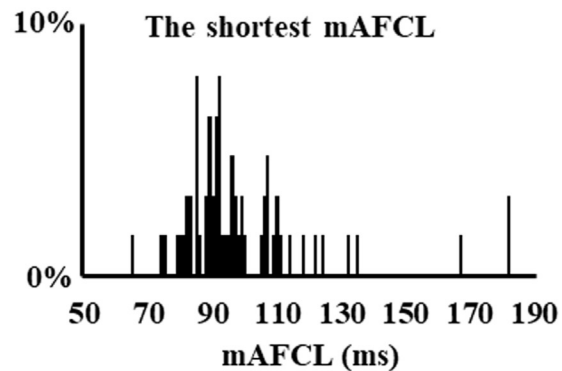


Figure 2

Spatial distribution of mAFCL_{min}. Table summarizing the shortest mAFCL (mAFCL_{min}) per atrial region, for each patient separately, color coded to indicate the distribution of mAFCL_{min} across the mapped regions, ranging from the longest (white) to shortest (dark red) mAFCL_{min}. As depicted in the histogram and bar chart, the mAFCL_{min} ranges from 65 to 183 ms (median, 93 ms) and is most frequently located at the PV area (PV 48%, BB 14%, LA 22%, RA 22%). BB = Bachman's bundle; LAVG = left atrial ventricular groove; mAFCL = median atrial fibrillation cycle length; PID = patient study identity; PV = pulmonary vein; RA = right atrium; SD AFCL = standard deviation of atrial fibrillation cycle length; X = adequate signal-to-noise ratio for annotations was present in <3 distinct atrial regions; therefore, the patient is excluded from the mAFCL_{min} analysis.

SD AFCL

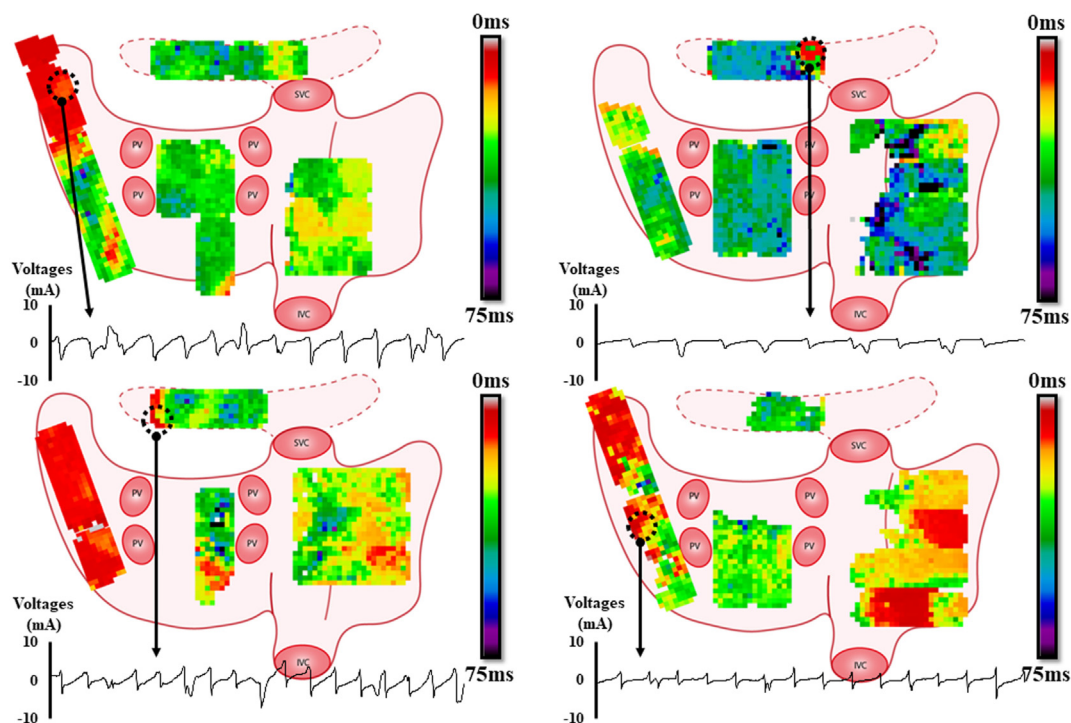


Figure 3

Distribution of SD AFCL in 4 patients. Schematic representation of the atria depicting the SD AFCL for each recording site separately, for the same 4 patients as depicted in Figure 1. Areas of regular activation may be found in a single or multiple atrial regions. Dotted circles indicate the smallest standard deviation site. Samples of EGM recordings from each smallest standard deviation site are displayed for each patient (duration 2 seconds). These EGMs mainly consist of single potentials and are not located at the same site or even mapping region as the corresponding shortest median AFCL in Figure 1. IVC = inferior caval vein; PV = pulmonary veins, SD AFCL = standard deviation of atrial fibrillation cycle length; SVC = superior caval vein.

mAFCL at sites of maximum repetition was 156 ms and ranged from 86 to 245 ms, which was not shorter than mAFCL at the remaining recording sites (155 [110–243] ms; uncorrected $P = .042$). SD AFCL ranged from 7 to 67 ms (median, 27 ms) and was smaller than at other recording sites (SD, 36 [range, 14–57] ms; $P < .001$).

At recording sites with maximum repetition, electrogram complexity differed slightly from other recording sites, given that they contained a larger proportion of short double potentials (19% [14%–25%] vs 16% [14%–18%]; $P < .001$).

Interestingly, re-entrant activation was not detected in any of the AF recordings.

Discussion

In this study, we investigated patterns of activation underlying high fibrillatory rates and regularly activated atrial areas on a high-resolution scale by performing elaborate mapping of both atria including Bachmanns bundle in patients with different AF subtypes. Recording sites harboring the highest fibrillatory rates were often located at the pulmonary vein area and showed a relatively high cycle length irregularity. At these sites, fibrillation waves with CB occurred as the most frequent pattern of activation, corresponding to higher proportions of electrogram fractionation. In contrast, the most regularly activated areas predominantly occurred along

the LAVG and corresponded to relatively high numbers of smoothly propagating waves and single potentials. We detected a series of at least 2 consecutive focal fibrillation waves in all patients, but zero occurrences of rotational activity. The right atrium and LAVG were the most prominent predilection sites for a series of repetitive focal fibrillation waves. These predilection sites for focal activation patterns were not identified by locating the mAFCL_{min} or the SD_{min} AFCL. These findings do not support the concept of targeting recording sites based on the mAFCL_{min} or the most regular activation alone.

Gold standard mapping technique

The rationale for identifying fast and regular activation is derived from the hypothesis that AF is driven by temporally stable drivers such as ectopic foci or rotational activity. These drivers should give rise to fast and regular local activation nearby or at the origin of fibrillation waves, degrading into irregular fibrillatory activity in atrial regions more distal from the driver. In previous studies, short AFCL and AFCL regularity were typically inferred from automated algorithms designed to facilitate the assessment of numerous electrograms.^{4,7,22} These algorithms perform variably with respect to frequency assessment in rhythms with increased interval irregularity and electrogram fractionation.²³ In addition, there is poor correlation between the organization index of a frequency

PID	RA	BB	LAVG	PV
1	X	X	X	X
2	36	22	13	19
3	32	8	8	9
4	10	18	8	11
5	7	16	15	25
6	13	12	9	16
7	49	19	15	19
8	16	13	12	15
9	11	10	10	19
10	12	1	7	
11	18	20	13	15
12	8	18	7	
13		15	2	6
14	14	16	16	20
15	22	12	10	12
16		17	3	28
17	3	7	4	5
18		4	3	3
19	3	2	11	12
20	17	11	9	17
21	23	17	7	15
22	11	11	17	13
23		8	9	14
24	35	13	12	
25	26	2		19
26	19	12	23	13
27	9	9	8	12
28	18	6	8	
29	18	17	7	13
30	17	9	14	6
31	X	X	X	X
32	11	17	14	11
33	10	14	9	12
34	21	15	11	13
35	6	13	11	13
36	12	11	7	5
37	10	15	12	22
38	19	15	10	9
39	16	22	11	15
40	25	17	11	17
41	27	18		14
42	11	20	8	13
43	X	X	X	X
44	7	7	4	11
45	13	4	13	30
46	13	14	10	36
47		15	13	24
48	19	13	18	
49	15	12	11	11
50	X	X	X	X

PID	RA	BB	LAVG	PV
51	10	15	13	8
52	6	11	7	11
53	16	10	9	12
54	18	23	8	8
55	20	5	2	27
56	3	14	5	10
57	15	7	9	17
58	2	13	1	8
59	15	13	19	15
60	22	20	14	9
61	X	X	X	X
62	28	17	9	
63		11	9	
64		20	4	10
65	14	11		
66	16	16	13	12
67	X	X	X	X
68		15	6	13
69	9	13	13	9
70	7	9	4	14
71	3	2		1

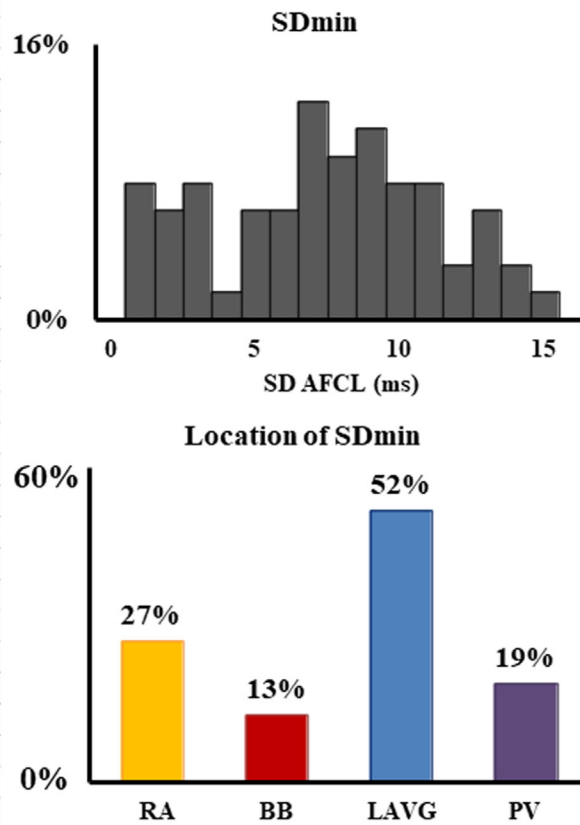


Figure 4

Spatial distribution of SD_{min}. Table summarizing the shortest SD_{min} per atrial region, for each patient separately, to identify the most regularly activated areas. The histogram and bar chart, respectively, show that SD_{min} ranges from 1 to 15 ms (median, 9 ms) and is most frequently located along the LAVG (LAVG 52%, BB 13%, PV 19%, RA 27%). In 7 patients, 2 distinct regions both displayed the most regularly activated sites. Areas harboring the most regularly activated areas do not correspond to areas harboring the fastest activated sites displayed in Figure 2. PID = patient study identity; PV = pulmonary veins; RA = right atrium; SD AFCL = standard deviation of atrial fibrillation cycle length; SD_{min} = smallest standard deviation of AFCL in the entire atria; X = adequate signal-to-noise ratio for annotations was present in <3 distinct atrial regions; therefore, the patient is excluded from the SD_{min} analysis.

Table 2 Patterns of activation at recording sites of interest

Recording site	Focal (%)	Smooth (%)	CB (%)	Collision (%)	Remnant (%)
mAFCL _{min}	2 [1–3]	3 [0–7]	81 [76–85]	0 [0–0]	13 [7–20]
SD _{min}	0 [0–3]	33 [24–54]	64 [47–73]	0 [0–0]	1 [0–3]
Other recording sites	1 [0–2]	17 [11–25]	74 [68–76]	0 [0–0]	7 [5–10]

CB = fibrillation waves with inter- or intrawave conduction block; Focal = fibrillation waves with focal pattern of activation; mAFCL_{min} = recording site with the shortest median atrial fibrillation cycle length in the atria; SD_{min} = recording site with the smallest standard deviation of atrial fibrillation cycle length in the atria; Smooth = smoothly propagating fibrillation waves.

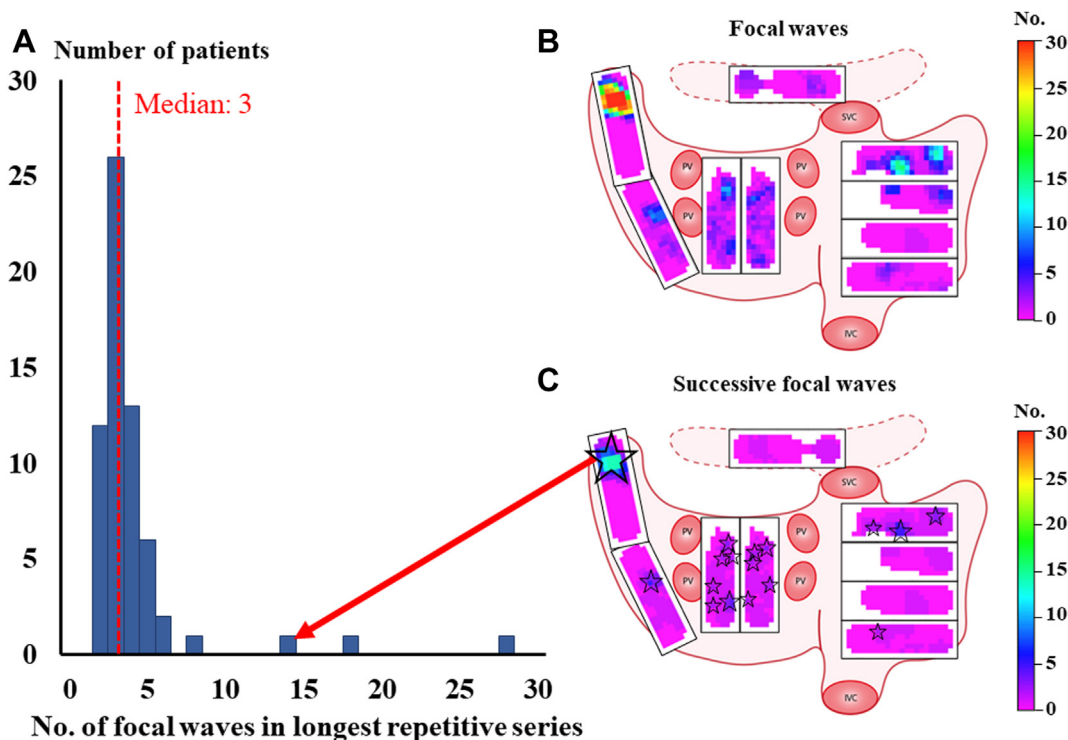
distribution used to quantify AFCL irregularity and the SD of manually computed AFCL.²⁴ Unique for this field of study is that we used direct and manually checked measures of AFCL and AFCL regularity during elaborate mapping on a high-scale spatial resolution and thereby avoided issues inherent to automated signal processing.

Perspective on rotational activity

Atrial regions activated at short or regular cycle lengths were assessed in this study to investigate the relation among activation frequencies, AFCL regularity, and repetitive patterns of activation reflecting the AF substrate. Neither mAFCL_{min} nor

SD_{min} was found at the core of re-entry circuits or at the origin of repetitive focal fibrillation waves.

There is ongoing debate with respect to the prevalence of rotors and foci in human AF, given that the occurrence and stability of these activation patterns vary strongly among different mapping approaches.² Previous high-density epicardial mapping studies typically also either failed to demonstrate re-entry^{18,19} or reported transient rotational wavefronts in a small minority of patients.^{13,25,26} However, in a small patient population of 10 patients with longstanding persistent AF, Walters and colleagues²⁷ repetitively recorded 10 seconds of AF over a total period of 10 minutes and detected transient rotors in 9 of 10 patients with a median

**Figure 5**

Repetitive focal patterns of activation. **A:** Histogram summarizing for the entire patient group the maximum length of a series of repetitive focal fibrillation waves. In all patients, at least 1 series of ≥ 2 consecutive focal fibrillation waves was detected; the median number of consecutive focal fibrillation waves in the longest series of focal fibrillation waves was only 3. In 1 patient, the maximum number of repetitive focal fibrillation waves was 28. **B:** Schematic overview of the occurrence of focal fibrillation waves throughout the atria in 1 exemplary patient. For each recording site separately, the total number of focal fibrillation waves occurring during 10 seconds is depicted in color code. In this case, focal fibrillation waves occurred at all mapping locations and frequently occurred more than once at the same recording site. However, the highest incidence of focal fibrillation waves occurred at the LA appendage. **C:** Schematic overview of the atria showing only the longest series of consecutive focal fibrillation waves for each recording site, for the same patient as in panel B. Recording sites are marked with a star if the longest series of focal fibrillation waves was at least 2. The star size is related to the number of focal fibrillation waves in the longest series. In this patient, the longest series of consecutive focal fibrillation waves was 14 (located at the LA appendage), length of all other maximum series ranged from 2 to 5 consecutive focal fibrillation waves. However, most focal fibrillation waves occurred as isolated events, even though the incidence of focal waves during the entire recording may be more than 1 at the corresponding recording sites in panel B.

duration of 3 rotations. Although we focused on detecting temporally stable rotors and focal patterns of activation by identifying the sites that were fastest activated and most regularly activated, we investigated all patterns of activation at >90,000 recording sites during 10 seconds and could not confirm a single case of stable or transiently rotating fibrillation waves. Besides the use of bipolar recordings, the methodology of Walters and colleagues²⁷ is highly similar to the methodology applied in our current study, and it remains unclear why the outcomes of both studies are contradictory. Given that they reported an average re-entrant core covering 4 ± 3 bipoles (interelectrode distance, 2.5 mm), it seems unlikely that our mapping arrays were too small to capture a rotational core at least once in the entire population.

Endocardial mapping studies with lower spatial resolution that investigated rotors and foci through detecting dominant frequencies, phase singularities, or undisclosed algorithms⁷ reported multiple temporally stable rotors and focal activation patterns in most patients.²² In contrast, panoramic, noncontact mapping studies typically report that foci and rotors are all transient in nature. Neither of these outcomes was confirmed in our current study.

However, something the mapping techniques do have in common is the predilection site for rotor detection at the LA. Likewise, we frequently detected focal activation patterns along the LAVG. It is possible that similar activation patterns have been interpreted differently owing to differences in spatial recording resolutions. For example, as previously explained in detail by Berenfeld,²⁸ it is possible that focal patterns of activation assessed with low spatial resolution may lead to false-positive rotational activity, given that focal waves appearing in between widely spaced electrodes may reach the surrounding recording sites at different times, hence giving the impression of wavefront rotation.

Why do repetitive focal fibrillation waves occur?

The focal patterns of activation as detected in our study population may be explained by various underlying mechanisms; however, owing to the study design, it is not possible to determine the exact cause. In a recent study, Hermans and colleagues¹³ propose a method on how to select from all recordings the most regular repetitive focal and rotational activation patterns—repetitive defined as >2 repetitions or rotations, respectively. From biatrial AF recordings in 13 patients (Penta Ray catheter, LAT mapping), the relatively most regular driver-like activation patterns were identified in 10 sites in 7 patients, although only in 1 patient was a significant entrainment of these repetitive activation patterns observed. It was proposed that these focal activation patterns may be attributed to an AF driver, although causality could not be demonstrated. However, it is not always clear how focal fibrillation waves acting as drivers, should be distinguished from focal fibrillation waves emerging after a fibrillation wave crosses intramural connections. Although no official consensus exists on the definition of *repetitive* focal fibrillation waves, a minimum of 2 consecutive focal waves has

been used to identify driver-like activation and consequently target these sites during ablation of AF in previous clinical studies.²¹ In all our patients, repetitive focal fibrillation waves meeting this criterion were detected at least once. It seems unlikely that an atrial site displaying only 2 focal fibrillation waves during the entire recording plays a pivotal role in AF persistence, unless multiple dispersed foci are active during the same period and only a low number of repetitions per site is necessary to maintain the fibrillatory process. In this study, the maximum total number of focal fibrillation waves occurring at 1 recording site was 10 (3–50) for each patient, indicating a high probability of recurrence of focal activation patterns within 10 seconds even though they may not occur as a continuous series.

As in this high-density mapping study, neither the recording sites with the maximum number of repetitive focal fibrillation waves nor the maximum proportion of focal fibrillation waves were identified at sites with the shortest AFCL or the lowest SD; it is unlikely that these focal waves were driving the fibrillatory process. Therefore, focal fibrillation waves present within this study population appear more consistent with endoepicardial breakthrough waves.

These breakthrough sites may be anatomically determined. In an experimental study, researchers found that conduction from the pulmonary veins across the ligament of Marshall led to focal patterns of activation at the LA epicardium.²⁹ This would explain why we found atrial areas that were more regularly activated than atrial tissue showing repetitive focal patterns of activation. Owing to the inherent anatomic variation of the pericardial reflection at the LA and pulmonary veins, it is unlikely that our mapping array covers the full extent of pulmonary muscular sleeves. Therefore, ectopic activity arising from the pulmonary veins muscular sleeve may not have been recognized as focal fibrillation waves because they were bound to be located out of sight or intersecting the border of the mapping array. If ectopic sources were indeed located in the pulmonary veins muscular sleeves, linking of fibrillation waves appearing from the pulmonary veins regions should have occurred. We did not observe this; however, we also did not systematically quantify the degree of linking of fibrillation waves throughout the atria.

Impact of the refractory period on the detection of AF drivers

We did not find any evidence for repetitive rotational patterns of activation in the entire study population. Rotational activation may have been missed if the center of the re-entrant circuit exceeded the dimensions of our mapping array or if re-entry occurred within 50 ms, owing to the blanking period applied during automated data processing. However, there is no evidence that reexcitation of cardiomyocytes can occur within 50 ms,¹⁷ and therefore, refractory periods shorter than 50 ms are not implemented in any mapping study published so far, except for during studies where the degree of fractionation rather than fibrillation rate is investigated.³⁰ In a previous epicardial mapping study, it was reported that

87% of transient rotational activity occurred in areas with AFCL shorter than 100 ms, where they also applied a refractory period of 50 ms for electrogram annotations.²⁷

Limitations

It is not possible to determine the exact cause of the focal fibrillation waves detected in this study population from sequential epicardial mapping, given that global coverage is not possible and the full trajectory of fibrillation waves can therefore not be observed. The arrhythmogenic substrate of our patient group does not necessarily represent the AF substrate in patients without structural heart disease. However, the occurrence of focal and re-entrant activation was also reported in patients with permanent AF admitted for surgical correction of mitral valve disease, suggesting that patients with and without structural heart disease at least partly share AF substrate characteristics.³¹ In this study, differences between epicardial and endocardial recordings were not investigated. However, in a previous work, we demonstrated that patterns of activation occurring within a specific period are comparable between the endocardial and epicardial layers¹⁹; therefore, patterns of epicardial activation are also translatable to the endocardium.

Conclusion

During extensive mapping, the fastest or most regularly activated areas are characterized by CB and smoothly propagating waves instead of repetitive occurrence of focal or rotational patterns of activation. The findings of our study have a direct impact on clinical practice, given that rotors are usually detected by identifying the fastest or most regularly activated recording sites. However, these sites do not correspond to repetitive occurrence of focal or rotational patterns of activation. This observation indicates the necessity of other parameters that accurately identify driver sites. It is generally assumed that CB areas play an important role in initiation and perpetuation of AF.³² Recently, it has been demonstrated that the number of functional CB areas is a predictor of AF recurrences after PV isolation. Given that the fastest activated sites in our study harbored CB areas, it could indicate that the mAFCL_{min} is an indicator of potential target sites for substrate-based AF ablation approaches. Future studies will have to demonstrate whether CB areas are indeed true AF perpetuators and hence suitable target sites for antiarrhythmic therapy.

Appendix

Supplementary data

Supplementary data associated with this article can be found in the online version at <https://doi.org/10.1016/j.hrthm.2025.05.024>.

Acknowledgments

The authors kindly thank J.A. Bekkers, MD, PhD; W.J. van Leeuwen, MD; F.B.S. Oei, MD, PhD; P.C. van de Woestijne, MD;

F.R.N. van Schaagen, MD; Y.J.H.J. Taverne, MD, PhD; A. Yaksh, MD, PhD; C.P. Teuwen, MD, PhD; E.A.H. Lanfers, MD, PhD; E.M.J.P. Mouws, MD, PhD; J.M.E. van der Does, MD, PhD; R. Starreveld, MSc; C. Houck, MD, PhD; C.S. Serban, DVM; A. Heida, MD; W.F.B. van der Does, MD; Ramdat Misier, BSc; and M.C. Roos-Serote, PhD for their contribution to this work.

Funding Sources: N.M.S. de Groot is supported by funding grants from Dutch Research Council Vidi (grant number 91717339), Biosense Webster (ICD 783454), Medical Delta, and Circular NWO (NWA.1389.20.157).

Data Availability: The data underlying this article will be shared on reasonable request to the corresponding author.

Disclosures: The authors have no conflicts of interest to disclose.

Address reprint requests and correspondence: Dr Natasja M.S. de Groot, Translational Electrophysiology Unit, Department of Cardiology, Erasmus Medical Center, Dr. Molewaterplein 40, 3015GD Rotterdam, The Netherlands. E-mail address: n.m.s.degroot@erasmusmc.nl

References

1. Clarnette JA, Brooks AG, Mahajan R, et al. Outcomes of persistent and long-standing persistent atrial fibrillation ablation: a systematic review and meta-analysis. *Europace* 2018;20:f366–f376.
2. Lau DH, Linz D, Sanders P. New findings in atrial fibrillation mechanisms. *Card Electrophysiol Clin* 2019;11:563–571.
3. Nademane K, McKenzie J, Kosar E, et al. A new approach for catheter ablation of atrial fibrillation: mapping of the electrophysiologic substrate. *J Am Coll Cardiol* 2004;43:2044–2053.
4. Sanders P, Berenfeld O, Hocini M, et al. Spectral analysis identifies sites of high-frequency activity maintaining atrial fibrillation in humans. *Circulation* 2005;112:789–797.
5. Haissaguerre M, Hocini M, Denis A, et al. Driver domains in persistent atrial fibrillation. *Circulation* 2014;130:530–538.
6. Benharash P, Buch E, Frank P, et al. Quantitative analysis of localized sources identified by focal impulse and rotor modulation mapping in atrial fibrillation. *Circ Arrhythm Electrophysiol* 2015;8:554–561.
7. Verma A, Sarkozy A, Skanes A, et al. Characterization and significance of localized sources identified by a novel automated algorithm during mapping of human persistent atrial fibrillation. *J Cardiovasc Electrophysiol* 2018;29:1480–1488.
8. Verma A, Jiang CY, Betts TR, et al. Approaches to catheter ablation for persistent atrial fibrillation. *N Engl J Med* 2015;372:1812–1822.
9. AtriENZA F, Almendral J, Ormaetxe JM, et al. Comparison of radiofrequency catheter ablation of drivers and circumferential pulmonary vein isolation in atrial fibrillation: a noninferiority randomized multicenter RADAR-AF trial. *J Am Coll Cardiol* 2014;64:2455–2467.
10. Podziemiński P, Zeemering S, Kuklik P, et al. Rotors detected by phase analysis of filtered, epicardial atrial fibrillation electrograms colocalize with regions of conduction block. *Circ Arrhythm Electrophysiol* 2018;11:e005858.
11. Quintanilla JG, Perez-Villacastin J, Perez-Castellano N, et al. Mechanistic approaches to detect, target, and ablate the drivers of atrial fibrillation. *Circ Arrhythm Electrophysiol* 2016;9:e002481.
12. Honarbakhsh S, Schilling RJ, Providencia R, et al. Characterization of drivers maintaining atrial fibrillation: correlation with markers of rapidity and organization on spectral analysis. *Heart Rhythm* 2018;15:1296–1303.
13. Hermans BJM, Ozgul O, Wolf M, et al. Selecting repetitive focal and rotational activation patterns with the highest probability of being a source of atrial fibrillation. *J Mol Cell Cardiol Plus* 2024;7:100064.
14. Yaksh A, van der Does LJ, Kik C, et al. A novel intra-operative, high-resolution atrial mapping approach. *J Interv Card Electrophysiol* 2015;44:221–225.
15. van der Does L, Yaksh A, Kik C, et al. Quest for the arrhythmogenic substrate of atrial fibrillation in patients undergoing cardiac surgery (QUASAR study): rationale and design. *J Cardiovasc Transl Res* 2016;9:194–201.
16. Anderson RH, Back Sternick E, Mahmud R, et al. How best to describe the location of the substrates for abnormal cardiac rhythms. *Heart Rhythm* 2024;21:2377–2385.
17. van Staveren LN, de Groot NMS. Exploring refractoriness as an adjunctive electrical biomarker for staging of atrial fibrillation. *J Am Heart Assoc* 2020;9:e018427.
18. Allesie MA, de Groot NM, Houben RP, et al. Electropathological substrate of long-standing persistent atrial fibrillation in patients with structural heart disease: longitudinal dissociation. *Circ Arrhythm Electrophysiol* 2010;3:606–615.

19. de Groot NM, Houben RP, Smeets JL, et al. Electropathological substrate of long-standing persistent atrial fibrillation in patients with structural heart disease: epicardial breakthrough. *Circulation* 2010;122:1674–1682.
20. de Groot NMS, Kleber A, Narayan SM, et al. Atrial fibrillation nomenclature, definitions, and mechanisms: position paper from the international Working Group of the Signal Summit. *Heart Rhythm* 2024;22:1480–1491.
21. Lim HS, Denis A, Middeldorp ME, et al. Persistent atrial fibrillation from the onset: a specific subgroup of patients with biatrial substrate involvement and poorer clinical outcome. *JACC Clin Electrophysiol* 2016;2:129–139.
22. Swarup V, Baykaner T, Rostamian A, et al. Stability of rotors and focal sources for human atrial fibrillation: focal impulse and rotor mapping (FIRM) of AF sources and fibrillatory conduction. *J Cardiovasc Electrophysiol* 2014;25:1284–1292.
23. Ng J, Kadish AH, Goldberger JJ. Effect of electrogram characteristics on the relationship of dominant frequency to atrial activation rate in atrial fibrillation. *Heart Rhythm* 2006;3:1295–1305.
24. Lee S, Ryu K, Waldo AL, Khrestian CM, Durand DM, Sahadevan J. An algorithm to measure beat-to-beat cycle lengths for assessment of atrial electrogram rate and regularity during atrial fibrillation. *J Cardiovasc Electrophysiol* 2013;24:199–206.
25. Lee G, Kumar S, Teh A, et al. Epicardial wave mapping in human long-lasting persistent atrial fibrillation: transient rotational circuits, complex wavefronts, and disorganized activity. *Eur Heart J* 2014;35:86–97.
26. Konings KT, Kirchhof CJ, Smeets JR, Wellens HJ, Penn OC, Allessie MA. High-density mapping of electrically induced atrial fibrillation in humans. *Circulation* 1994;89:1665–1680.
27. Walters TE, Lee G, Morris G, et al. Temporal stability of rotors and atrial activation patterns in persistent human atrial fibrillation: A high-density epicardial mapping study of prolonged recordings. *JACC Clin Electrophysiol* 2015;1:14–24.
28. Berenfeld O, Oral H. The quest for rotors in atrial fibrillation: different nets catch different fishes. *Heart Rhythm* 2012;9:1440–1441.
29. Tan AY, Chou CC, Zhou S, et al. Electrical connections between left superior pulmonary vein, left atrium, and ligament of Marshall: implications for mechanisms of atrial fibrillation. *Am J Physiol Heart Circ Physiol* 2006;290:H312–H322.
30. Stiles MK, Brooks AG, Kuklik P, et al. High-density mapping of atrial fibrillation in humans: relationship between high-frequency activation and electrogram fractionation. *J Cardiovasc Electrophysiol* 2008;19:1245–1253.
31. Nitta T, Ishii Y, Miyagi Y, Ohmori H, Sakamoto S, Tanaka S. Concurrent multiple left atrial focal activations with fibrillatory conduction and right atrial focal or reentrant activation as the mechanism in atrial fibrillation. *J Thorac Cardiovasc Surg* 2004;127:770–778.
32. Frontera A, Vilella F, Cristiano E, et al. The Functional substrate in patients with atrial fibrillation is predictive of recurrences after catheter ablation. *Heart Rhythm* 2024;22:1401–1410.